Innovative non-destructive sorting technique for juicy stone fruits: textural properties of fresh mangos and purees

Paola Labaky [a, b, c], Lidwine Grosmaire [b], Julien Ricci [a], Christelle Wisniewski [b], Nicolas Louka [c], Layal Dahdouh [a]

a. CIRAD, UMR Qualisud, F-34398 Montpellier, France.
b. Qualisud, Univ Montpellier, CIRAD, Montpellier SupAgro, Univ d'Avignon, Univ de La Réunion, Montpellier, France.
c. Université Saint Joseph de Beyrouth, Faculté des Sciences, Centre d'Analyses et de Recherche, Unité de Recherche Technologies et Valorisation Agro-alimentaire, Beyrouth, Liban.

Corresponding author: Layal Dahdouh [a], layal.dahdouh@cirad.fr, +33 (0)4 67 61 57 23
Cirad-Persyst,73 rue Jean-François Breton, 34398 Montpellier cedex 5

Abstract

Mango has an abundant production leading to important post-harvest losses. Mango processing is an alternative to reduce these losses. Nowadays, the lack of instrumental tools suitable to sort mangos according to their ability to be processed into products with specific quality is a main setback for their processing. The aim of this study was to develop new tools, mainly non-destructive, to sort easily fresh mangos according to their maturity stage and to the specific properties of their purees. To this end, an innovative experimental strategy combining textural, rheological and physico-chemical analyses was proposed to characterize mangos and their purees. Results showed that mango firmness is a great indicator of mango heterogeneity and has an important impact on the properties of mango purees. A non-destructive compression test was reliable to measure accurately mango firmness and to anticipate rheological and particles size properties of mango purees.

Abbreviations

D_{5N} and D_{10N}, distance of compression at 5 and 10 N (mm); DM, dry matter (g /100 g puree); D_{10}, particles size for which 10% of the particles have a size smaller than this diameter (µm);

D_{50}, particles size for which 50% of the particles are smaller than this diameter (µm); D_{90}, particle size for which 90% of the particles are smaller than this diameter (µm); D [3;2], surface area average diameter or Sauter mean diameter : the diameter of a sphere that has the same volume/surface ratio as the set of particles (µm); D [4;3], volume mean diameter or Brouckere mean diameter : the diameter of a sphere whose volume is equal to the average volumes of all the particles in the sample (µm); F_{max}, maximum value of the peak force (N); g, gravitational acceleration ($m.s^{-2}$); G', storage modulus (Pa); G'', loss modulus (Pa); K, the consistency index ($Pa.s^n$); n, the flow behavior index, pH, potential hydrogen; RH, relative humidity (%); rpm, revolutions per minute; TA, titratable acidity (g citric acid/100g puree); TSS, total soluble solids (°Bx); µ, dynamic viscosity (Pa.s).

Keywords

Mango, purees, texture, rheology, maturity, sorting tool

1. Introduction

Mangifera indica L. known as mango, is a tropical fruit originated from the Indo-Burmese region. Mango is one of the most produced (mainly in India, China, Thailand, Indonesia and Pakistan) and consumed fruits worldwide after banana (Chantalak and Robert E, 2017; Masud Parvez, 2016). There is a large variety of mangos that differ in size, color, texture, and nutritional properties. The most consumed mangos varieties are Kent, Keitt, Haden, Tommy Atkins, Cogshall, Alphonso, Amelie and Valencia pride (Djioua et al., 2010).

According to the FAO statistics, mango production worldwide increased by 26 million metric tons over a period of 17 years to reach 50 million metric tons in 2017 (FAO, 2019). In developing countries, post-harvest fruit losses due to the abundant mango production can be estimated up to 40% (Boateng, 2016; Memon et al., 2013). Hence, processing and transforming mangos into purees, juices, jams, canned products and dried slices (Evans et al., 2017) is an alternative not only to minimize post-harvest losses but also to provide local incomes. Nevertheless, the quality of processed products (physical, physico-chemical and organoleptic characteristics) depends on the maturity stage of raw mangos (Ellong et al., 2015). Indeed, the heterogeneity of the maturity stages encountered in a same batch of mangos for processing constitute a barrier for controlling the process and the quality of the finished product (Rivier et al., 2009)

In the light of the above, fruit sorting prior to mango processing is generally performed in processing units to reduce batch heterogeneity in relation with maturity stages. To date, mango sorting is mainly manual, time consuming and highly labor-dependent (visual and tactile know-how) leading in some cases to inaccurate fruits sorting and disparate quality of processed products. Several tools (e.g. textural, spectral, fluorescence and biochemical measurements) have been evaluated to predict the maturity stage or the quality of mango fruits (Pronprasit and Natwichai, 2013; Valente et al., 2011; Zakaria et al., 2012). However, as far as the authors are aware, in these studies, none of the proposed tools were conceived as to predict the quality of processed products.

Nowadays, the lack of instrumental tools suitable to sort mango fruits according to their ability to be processed into products with specific quality is a main setback for up-grading mango fruits. In this context, the aim of this work was to develop new methods and tools, mainly non-destructive, allowing to sort mangos according not only to their maturity stage but also to the specific properties of their processed products (puree). To this end, an experimental strategy combining mechanical (rheology and texture), physical and physico-chemical (particles size measurement, color, pH, titratable acidity, °Bx, dry matter) analyses was proposed to characterize fresh mangos and mango purees. Firstly, textural (penetrometry and compression), rheological (oscillatory), physical (weight, density) and color analyses were performed on fresh mangos at different stages of maturity. In a second place, fresh mangos were processed into purees that were characterized (particles size, rheology and physico-chemistry). Finally, statistical analyses were used to (i) identify pertinent instrumental indicators that describe the maturity stages of mangos, (ii) evaluate the impact of mangos maturity stage on purees characteristics and finally to (iii) propose new tools for sorting fresh mangos according to their ability to be processed into purees.

2. Materials and methods

2.1 Fruits

Fifty green mangos (*Mangifera indica* L., cv. Kent, Peru) previously stored at 10°C during 10 days (to slow down maturation) were purchased from a local warehouse (Georges Helfer SA, Plan d'Orgon, France). All mangos were stored in controlled conditions (18°C, 80% RH) between one and twenty-five days. Daily, one or two fruits were characterized. Each mango was transformed separately into puree and all measurements were carried out on the same fruit and its puree. Data of twenty-eight mangos were selected for this study.

2.2 Fresh mango characterization

Before the analyses, mango fruits, were soaked in chlorinated water (200 ppm sodium hypochlorite, Chem-Lab, Zedelgem, Belgium) and wiped with 70% ethanol (Honeywell, Riedel-de Haën, absolute, ≥ 99.9, Charlotte, North Carolina, USA) in order to remove the latex layer that covers the fruits (Palafox-Carlos et al., 2012; Penchaiya et al., 2015).

2.2.1 Fruit density

Fruit density was calculated using Archimedes' principle by measuring the fresh fruits mass in air and in water (each mango was placed in a basket hanging from the balance and fully immersed in water) according to the method described by Joas et al., 2009 (Joas et al., 2009).

2.2.2 Texture analysis

Firmness of mangos was measured using a texture analyzer (TA-XT2, Stable micro Systems, London, UK) equipped with a 5 kg load cell and an Exponent software (version 5.1.1.0) to record data.

Two different methods were evaluated: a non-destructive compression test and a destructive penetrometry test.

2.2.2.1 Non-destructive compression test

The compression test in this study was proposed to simulate the tactile perception of the operator during sorting mango fruits according to their firmness. Compression tests were performed on both larger sides of mango since water potential of the two sides may differ due to the position of the fruit on the tree and to its exposition to the sun. Measurements were performed on three different positions on each side of the fruit. The test was carried out to reach a maximum compression force of 10 N with a 2 cm spherical probe and probe speed of 1 mm.s^{-1}. The maximum force was carefully chosen in order to avoid damaging the fruit structure and subsequently proposing a non-destructive test. The obtained force-distance curves were recorded and the distances of compression (D_{5N} or D_{10N}) at 5 or 10 N were identified as the most consistent parameters to describe mango firmness. Similar results of D_{5N} and D_{10N} values were recorded regardless the side of mango ($R^2 > 0.99$) for linear correlations of D_{5N} data and D_{10N} data for side 1 and side 2 (data not shown). Considering this observation, results concerning compression tests will be presented only for D_{5N} and for one side in the following.

2.2.2.2 Destructive penetrometry test

Penetrometry test was performed on slices (h=15 mm, using an electric ham slicer generally used for processed meat) from each side of mango using a cylindrical stainless steel probe of 5 mm diameter. The test was carried out on the inner flesh tissue to reach a maximum distance of 5 mm with a probe speed of 1 mm.s^{-1}. The aim of this additional test was to evaluate the firmness of the mango flesh in a destructive way as it is conventionally done. The firmness of mangos was evaluated by the average of the maximum value of the peak force (F_{max}) of the resulting force-distance curves. Measurements were realized on three different positions of the slice.

2.2.3 Rheological measurements

Rheological measurements were carried out on cylindrical mango slices (2 mm thickness and 35 mm diameter) cut using an electric ham slicer generally used for processed meat.

Rheological measurements were performed using a Haake Mars 60 rheometer (Thermofisher, Waltham, Massachusetts, USA) equipped with a 35 mm serrated parallel plates geometry and a "RheoWin" software (version 4.82.0002) to record rheological data. A strain amplitude sweep test was performed in low strain amplitude range (from 0.01 to 1%) at a constant frequency of 1 Hz and a controlled normal force of 4 N. All experiments were conducted at temperature of 25°C ± 0.1 controlled by a Peltier system. The storage modulus values G'(Pa) at 0.1% of strain were selected as rheological indicator reflecting the solid-like behavior of mango slices. Measurements were performed in quadruplicate.

2.2.4 Flesh color

Color was determined on grinded flesh using a Minolta CR-300 colorimeter (Konica Minolta Sensing, Inc, Ramsey, New Jersey, USA) according to the CIELAB color system (L*, a*, b*). L* represents the lightness varying from 0 to 100, (0 representing black and 100 representing white), a* represents the variation from green (-) to red (+) and the b* reflects the variation from blue (-) to yellow (+).

2.3 Characterization of mango puree

2.3.1 Puree preparation

Each mango was manually peeled, the seed was removed and the flesh was cut into small pieces (around 1 cm^3). The flesh was grinded at 25°C with a Thermomix (Vorwerk, Typ 31-1, Wuppertal, Germany) at a speed of 1000 rpm for 1 min, 7000 rpm for 1 min and 10000 rpm for 2 min. After grinding, the puree (approximately 180g) was stored at 4°C before the analyses.

2.3.2 Rheological measurements

2.3.2.1 Rotational measurements

Rotational measurements of mango purees were performed using a Physica MCR301 rheometer (Anton Paar Gmbh, Graz, Austria) equipped with "Start Rheoplus" software (version RHEOPLUS/32 V3.40) to record the rheological data. A six blades vane geometry (ST22- 6V- 16, radius of 22 mm) was used with stationary cup with a radius of 27 mm giving a gap of 2.5 mm. The shear rate varied from 0.1 to 500 s^{-1} and temperature was held at 25°C ±

0.1 using a Peltier system. The evolution of dynamic viscosity μ (Pa.s), of each mango puree, as function of the shear rate $\dot{\gamma}$ (s^{-1}) was recorded.

2.3.2.2 Oscillatory measurements

Strain amplitude sweep tests were conducted using the Haake Mars 60 rheometer equipped with a 35 mm serrated parallel plates geometry. Frequency was held constant at 1 Hz, while strain amplitude varied between 0.01 and 100%. All experiments were conducted at a temperature of 25°C ± 0.1 controlled by a Peltier system. For each puree, the storage and loss moduli G' and G" were recorded as function of the strain (%). The values of the storage G' (Pa) and loss G" (Pa) moduli (at 1% of strain in the linear viscoelastic domain) were selected as rheological indicators reflecting the solid-like behavior and liquid-like behavior of mango purees, respectively.

2.3.3 Particles size measurements of suspended insoluble solids

Particles size distribution was determined by LASER diffraction using a Malvern Mastersizer (Mastersizer 3000, Malvern Instruments Limited, Worcestershire, UK). This particles size analyzer can provide theoretically particles size distribution from 10 nm to 3500 µm. Measurements were carried out in a wet-mode using distilled water as the suspension medium. The values 1.73 and 1.33 were used for the refractive indices of cloud particles and dispersion phase (water), respectively, and 0.1 was used for the absorption index of cloud particles (Dahdouh et al., 2016). Samples were introduced into the volume presentation unit, which already contained deionized water (obscuration of 20%). In this unit, the diluted sample was stirred at 1500 rpm and pumped through the optical cell. The initial particles size distribution of puree was verified to be not modified in such conditions of stirring and pumping. For each measurement, size distribution (volume density against particles size) was provided and statistical volume diameters, D_{10}, D_{50} and D_{90} were given (D_x indicates a particles size for which x% of the particles are below that size). The surface area average diameter D [3;2] (Sauter mean diameter) and the volume mean diameter D [4;3] (Brouckere mean diameter) were also provided (Dahdouh et al., 2015).

The D [3;2] indicates the diameter of a sphere that has the same volume/surface ratio as the set of particles Eq. (1):

$$D\,[3;2] = \frac{\sum_i n_i\, d_i^3}{\sum_i n_i\, d_i^2} \quad (1)$$

The D [4;3] indicates the diameter of a sphere whose volume is equal to the average volumes of all the particles in the sample Eq. (2):

$$D\,[4;3] = \frac{\sum_i n_i\, d_i^4}{\sum_i n_i\, d_i^3} \quad (2)$$

With n_i the number of particles of diameter d_i.

Particles size measurements performed separately on mango purees and on their isolated suspended insoluble solids (centrifugation 18000 g /30 min) provided identical particles size distributions, smaller compounds being not detectable in the Mastersizer operating conditions. Hence, results presented in this work concern mainly the particles size distribution of suspended insoluble solids (> 1µm) of purees.

2.3.4 Physico-chemical analyses

Mango is a climacteric fruit for which biochemical and nutritional changes occurring during tree-ripening can continue after harvesting. Titratable acidity (TA), total soluble solids (TSS) and dry matter (DM) were performed on purees according to protocols and methods used for fruit suspensions (Dahdouh et al., 2016). pH and titratable acidity were measured using an automatic Titroline apparatus (Schott Schweiz AG, St. Gallen, Switzerland). Titratable acidity was assessed by titration with 0.025 N NaOH until a pH 8.2. Titratable acidity (TA) was expressed in g of citric acid /100 g of puree since it is well known that citric acid is one of the major organic acids present in mango contributing to fruit acidity and flavor. Total soluble solids (TSS, expressed in °Bx) were measured with an Abbe refractometer (Atago, Japan). Dry matter (DM, expressed in g/100 g of puree) was determined by drying 3 g of puree at 70°C under vacuum for 24 h.

For all physico-chemical analyses, measurements were performed at 25°C in triplicate and the average values were used.

2.4 Statistical analyses

Multivariate analyses were carried out using XLSTAT (version 16.0.4744 Addinsoft, Paris, France). Principal component analysis (PCA), a multivariate projection method designed to reduce the dimensionality and to describe the variation of the data (Azira et al., 2014), was performed to analyze the total variability between samples and to identify groups with similar characteristics among fresh mangos and puree. Eight indicators for fresh mango (F_{max}, D_{5N}, G', L*, a*, b*, weight, density) and twelve indicators for purees (particles size: D [3;2], D [4;3], D_{10}, D_{50}, D_{90}; rheological behavior: G', G", K, n and physico-chemical characteristics:

TA, TSS and DM) were set as variables. The score plot was extracted from the first two principal components, PC 1 and PC 2, as they presented the maximum variability of the data.

3. Results and discussion

3.1 Fresh mangos

3.1.1 Texture characterization

Results regarding compression test are presented in Fig. 1(a). The distance achieved by the probe when applying 5 N (D_{5N}) on the raw mango increased significantly with maturation highlighting a significant loss of mango firmness. The loss of firmness of fruits occurring during the maturation period could be due to biochemical changes such as the degradation of pectins, cellulose and hemicellulose (Lawson et al., 2019; Padda et al., 2011; Yashoda et al., 2006).

Fig. 1(b) shows that the force (F_{max}) needed to puncture 15 mm of mango slice decreased significantly during maturation confirming the loss of firmness. However, penetrometry test seems to be less discriminating regarding mango firmness than compression test after 15 days of maturation. Indeed, a significant decrease of F_{max} (92%) was observed before 15 days of maturation whereas beyond this maturation stage the F_{max} was almost steady. After 15 days, the difference of the flesh firmness was not high enough to be detectable by the penetrometry test. Contrariwise, in the case of compression test, the firmness of the whole fruit (peel and flesh) was measured, leading to better results.

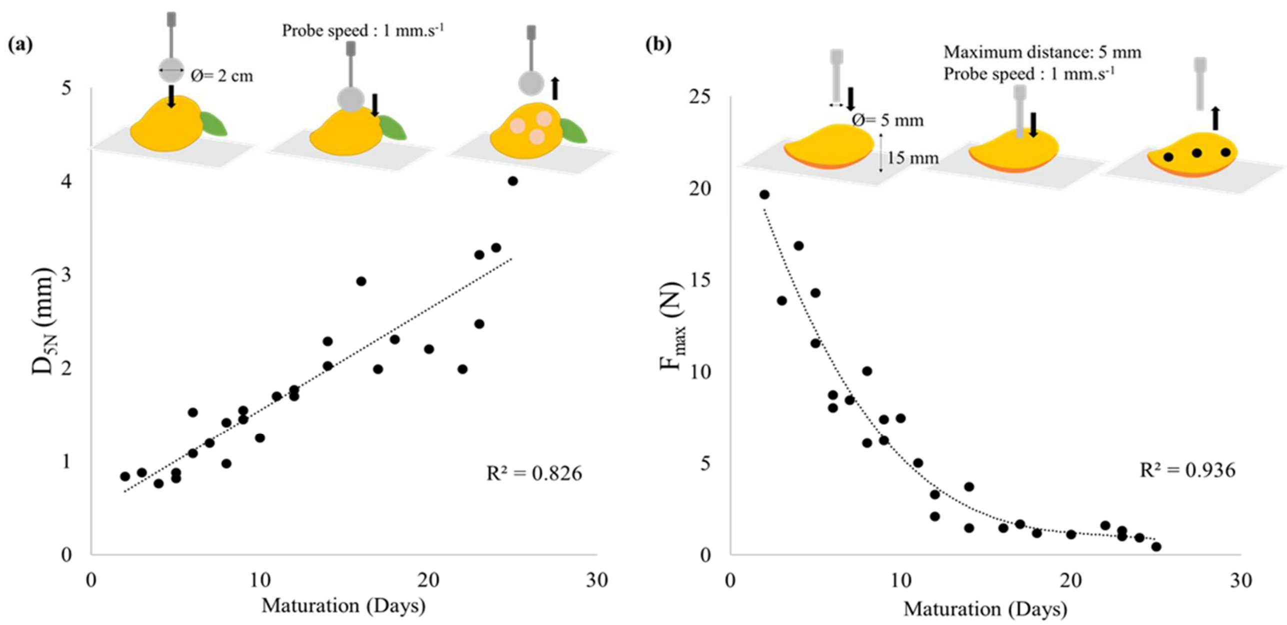

Fig. 1. Evolution of (a) D_{5N} (mm) and (b) F_{max} (N) during maturation.

3.1.2 Rheological characterization

Since texture tests showed that the firmness of mango flesh decreased during maturation, rheological measurements were performed to assess the evolution of the solid-like behavior of mango flesh in relation with firmness loss during maturation. To this end, the storage modulus G' (Pa) reflecting the solid-like behavior of a material was evaluated through oscillatory test in small amplitude range (0.1 to 1%) within the linear viscoelastic range (Lee, 2018).

Fig. 2 (a) depicts the evolution of the storage modulus G' (Pa) as function of maturation days showing that the solid-like behavior of mango flesh decreased significantly during maturation. Indeed, the storage modulus of mango slices at the end of maturation was 10 times lower than the one recorded for green mango at early maturation stages. This observation emphasizes that biochemical and physico-chemical phenomena (starch, cell wall, cellulose and hemicellulose degradation, etc.,) (Nambi et al., 2016) occurring during maturation led to a modification of the viscoelastic properties of mango flesh and subsequently to its loss of firmness.

Moreover Fig. 2 (b) and (c), point up interesting correlations between the solid-like behavior (G') of mango flesh and the firmness of mango flesh (F_{max}) and the firmness of the whole fruit (D_{5N}). It is important to notice that the D_{5N} is a better indicator than F_{max} regarding the solid-like behavior of mango flesh at stages of maturation above 10 days (when F_{max} < 5 N), Fig. 2 (b) and (c). This result confirms that it is possible to trace back the solid-like behavior of mango flesh by performing a simple and non-destructive compression test on the whole fruit.

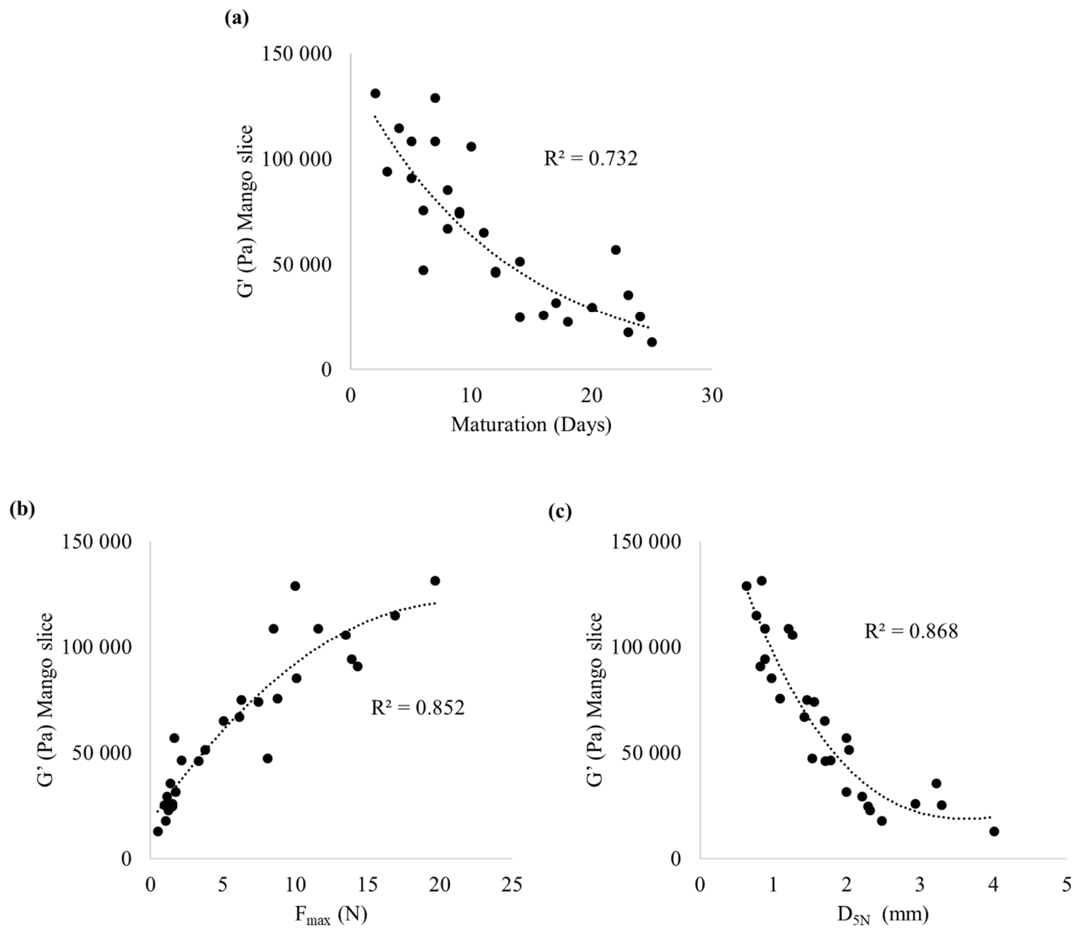

Fig. 2. Evolution of the storage modulus G' (Pa) of mango slices as function of (a) maturation (days), (b) F_{max} (N) and (c) D_{5N} (mm).

To sum up, both penetrometry (destructive) and compression (non-destructive) tests allowed to measure significant loss of mango firmness during maturation. Compression test provided better information about mango firmness after 15 days of maturation without damaging the fruits. Moreover, this simple and non-destructive compression test makes possible to trace back the solid-like behavior (G') of mango flesh, since D_{5N}, is a good indicator of the solid-like behavior of mango flesh even at stages of maturation above 15 days.

3.1.3 Other physical characterization: flesh color, fruit weight and density

Fruit weight, density and flesh color, were measured during maturation in order to assess the effect of maturation on these physical and physico-chemical characteristics of mangos (Gentile et al., 2018; Lawson et al., 2019).

Fruit density decreased during maturation as presented in Fig. 3(a). A weight loss of mango fruits during maturation is mentioned by Lawson et al., 2019 and explained by the loss of water through the stomata and pores (Lawson et al., 2019).

Concerning color, the variation of three parameters L*, a* and b* is generally used to monitor the variation of flesh color. The decrease of the lightness L* point up a darkening of fleshes during maturation due to the activity of the polyphenol oxidases forming brown pigments (Liu et al., 2013). The increase of a* and b* reveal biochemical changes (formation of carotenoids, chlorophyll degradation, etc.) during maturation (Lawson et al., 2019; Liu et al., 2013; Rumainum et al., 2018). In this study, the obtained results, Fig. 3 (b), (c), were similar to those previously reported by many authors regarding L* (L* was 1.2 times lower at the end of the maturation) and a* (a* was 7.4 times higher at the end of the maturation), but no significant evolution of b* was observed (Data not shown).

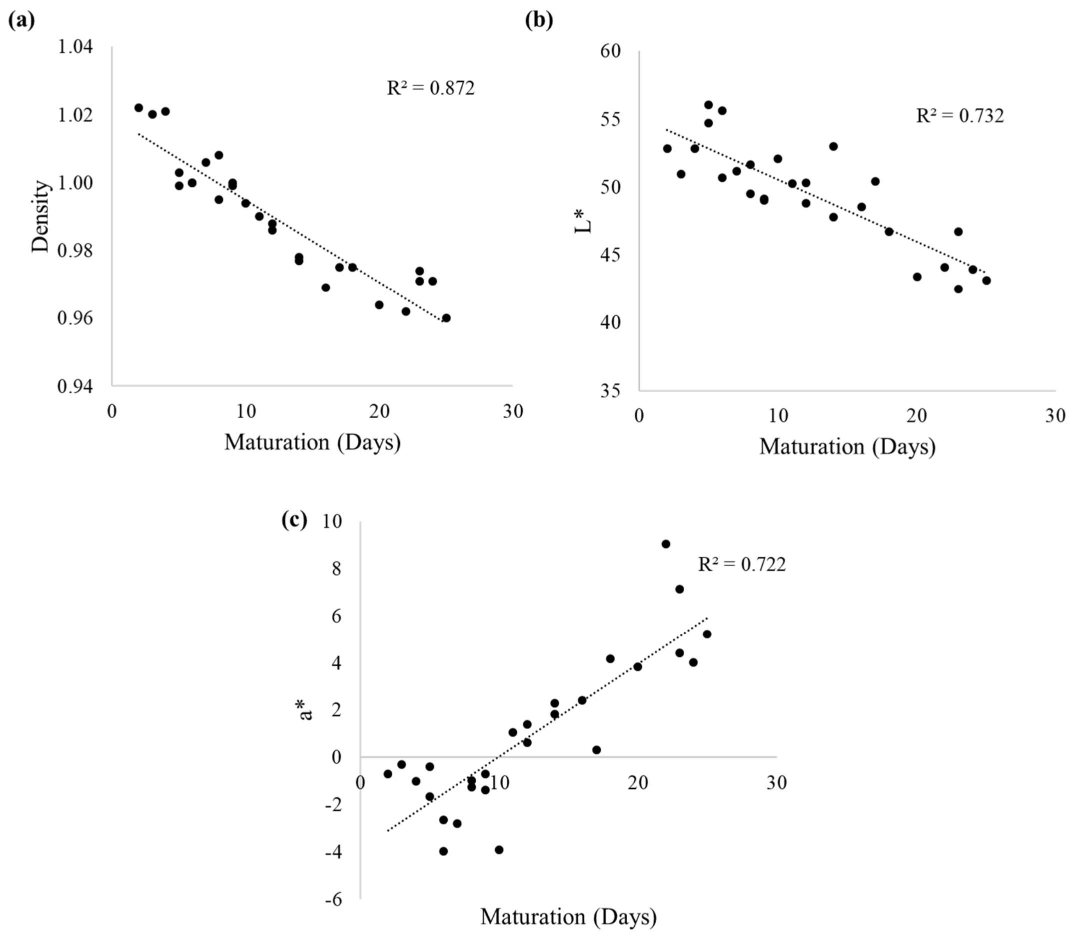

Fig. 3. Evolution of (a) density, (b) and (c) L*and a* (color parameters) during maturation (days).

3.2 Mango puree characterization and relations with fresh mangos characterization

3.2.1 Particles size of suspended insoluble solids

Fruit suspensions consist in two phases: a serum phase containing soluble compounds such as sugars, acids and soluble pectins and insoluble phase containing insoluble suspended solids such as pectins, fibers and cell walls fragments (Lopez-Sanchez et al., 2012). For fruits-based suspensions, it is well known that the concentration and the size of insoluble suspended solids have a major role in the structural and rheological characteristics of these products (Dahdouh et al., 2016). Therefore, particles size measurements were performed on mango purees to assess the size distribution of their suspended insoluble solids in relation with mango maturation stage and puree rheological properties. Fig. 4 presents examples of particles size distributions for mango purees at 5 different days of maturation. These distributions are typical of polydisperse suspensions with a monomodal size distribution as reported in the literature for many fruits suspensions such as apple purees and fruit juices (Dahdouh et al., 2016; Leverrier et al., 2016). It can be noticed that purees obtained from the greenest stage were characterized by the higher volume density for particles around 1000 µm. The volume density of these particles larger than 1000 µm decreased considerably as the stage of maturation increased to disappear in late stage of maturation. For purees obtained from mango beyond 10 days of maturation, the highest volume density for particles shifted from 1000 µm to 200 µm. Changes in particles size in purees in relation with mango maturation were also highlighted by the evolution of the statistical diameters as they all decreased significantly with maturation, Fig. 5 show some examples of the evolution of D_{10}, D_{50} and D [3;2] during maturation. Results concerning D_{90} and D [4;3] were not depicted in this section as they provided redundant information, they will be presented only in the statistical analyses.

This observation could be explained by the hydrolysis and degradation, during maturation, of large insoluble suspended solids (starch, pectins and cell walls) into smaller compounds leading to a decrease of the size of suspended insoluble particles (Venkatesan and Tamilmani, 2013). These results show that the loss of mango firmness and the hydrolysis of specific compounds (e.g. cell walls) during the maturation could lead to mango purees with smaller particles size.

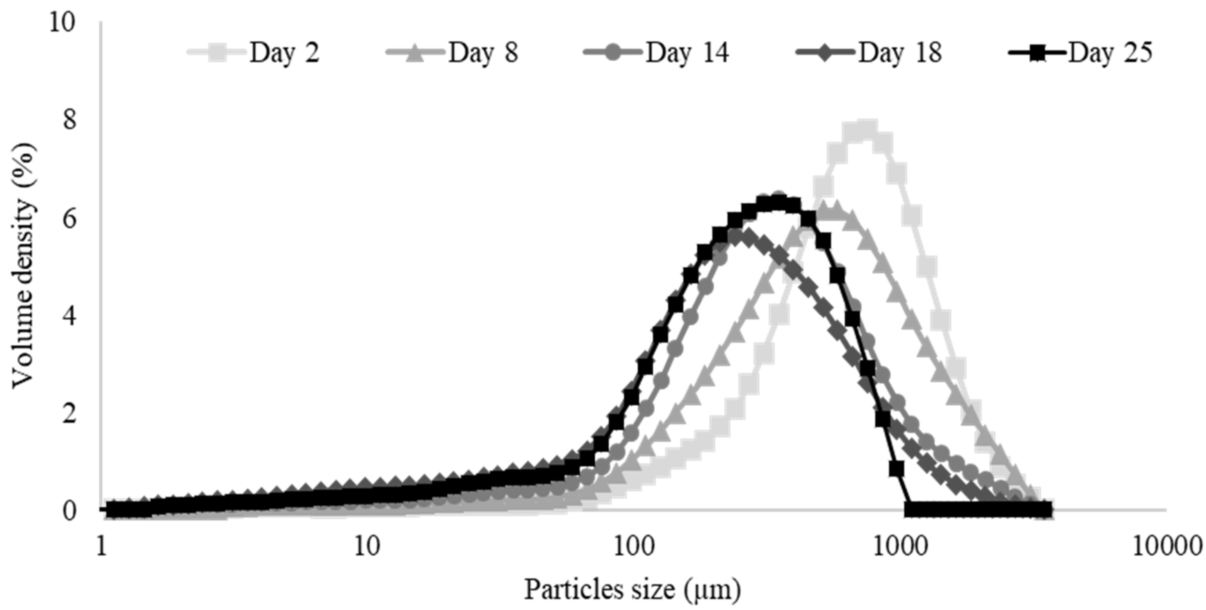

Fig. 4. Particles size distributions of mango purees at 5 different days of maturation.

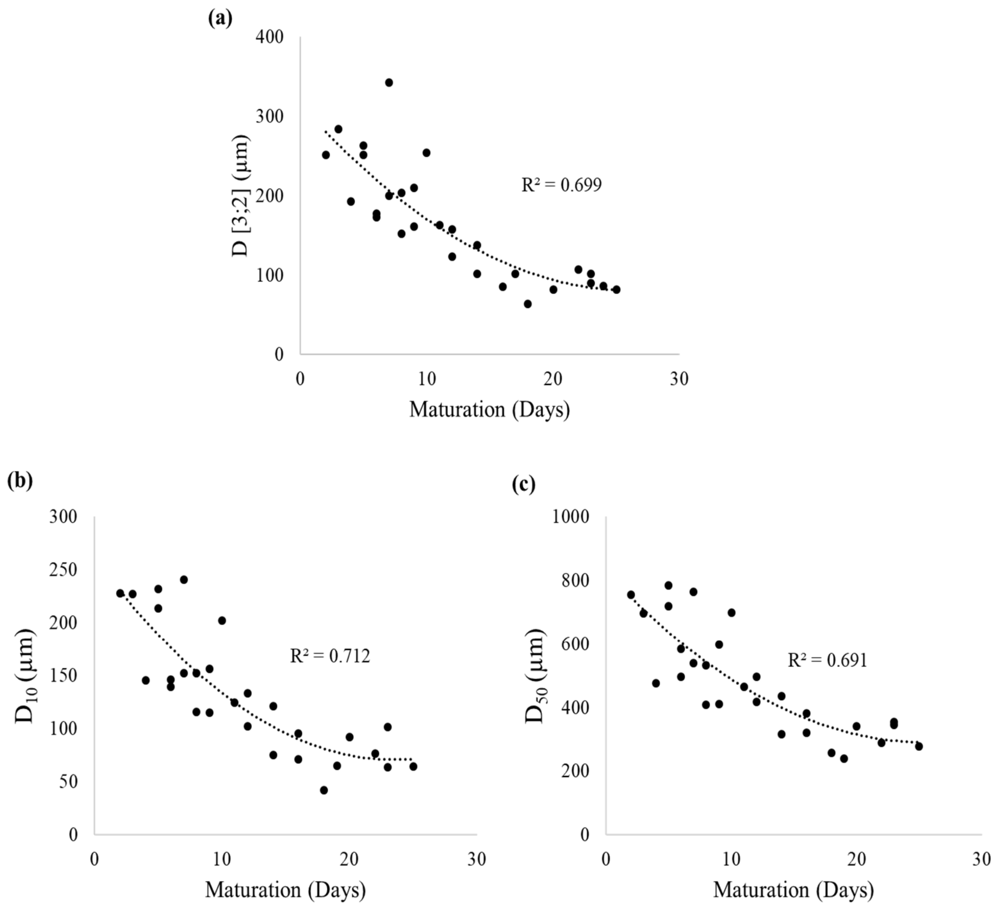

Fig 5. Effect of maturation on (a) D [3;2] (µm), (b) D_{10} (µm) and (c) D_{50} (µm).

Indeed, Fig. 6 (a), (b) point up significant correlations between the average surface diameter D [3;2] of the purees and the firmness of mango flesh (F_{max}) and the whole fruit (D_{5N}). These observations emphasize the impact of mango firmness on the particles size distribution of the puree. Moreover, the same trend is observed between the average surface diameter D [3;2] and the storage modulus G' of mango flesh on Fig. 6 (c), showing that particles size distribution of mango puree is closely dependent on the solid-like behavior of mango flesh. In fact, purees grinded from the greenest mangos with a higher storage modulus G' of the flesh presented purees with larger particles. Since it is well known that grinding conditions have an important impact on the particles size distribution of purees (Espinosa et al., 2011), standardized conditions of grinding were carefully used in this work, for all stages of maturation, allowing to show the specific role of mango firmness and solid-like behavior on the particles size of the purees. Hence, this work proposes for the first time a simple and fast tool to predict the particles size of mango purees (obtained in specific conditions) based on a non-destructive compression test (D_{5N}), since the same trends were observed when destructive texture and rheological analyses were performed.

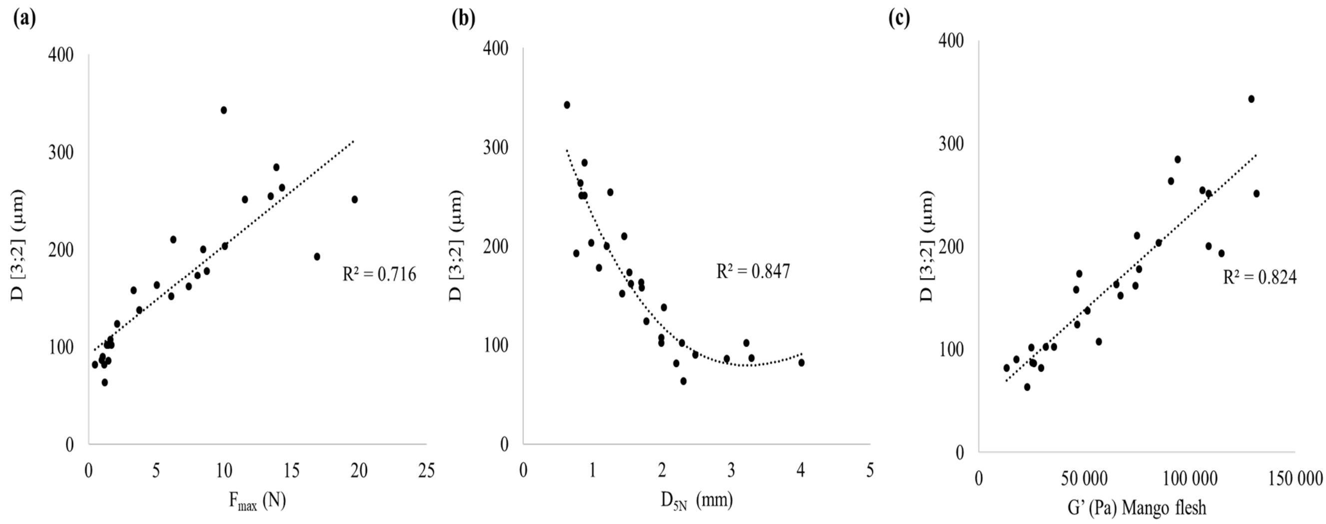

Fig. 6. Variation of the average surface diameter D [3;2] (µm) with (a) F_{max} (N), (b) D_{5N} (mm) and (c) G' of mango flesh (Pa).

3.2.2 Rheological characterization

3.2.2.1 Rotational measurements

The effect of maturation on the flow behavior of mango purees was investigated throughout the measurements of the viscosity of different mango purees. Several published studies, reported that fruits purees are characterized by shear-thinning behavior as their viscosity decreases with the increase of the shear rate (Espinosa-muñoz et al., 2013; Gundurao et al., 2011; Phaokuntha et al., 2014). Since all mango purees had also shear-thinning behavior in this study, a power Law (specific of this behavior) was used to determine the consistency index (K, Pa.s^n) and the flow behavior index (n) of each puree (with significant determination coefficient R^2, for $\alpha = 5\%$, degree of freedom = 27), Eq. (3):

$$\text{Power Law: } \mu_{mod} = K\dot{\gamma}^{n-1} \quad (3)$$

Where, μ_{mod}, the modeled viscosity (Pa.s), K, the consistency index (Pa.s^n), n, the flow behavior index and $\dot{\gamma}$ the shear rate (s^{-1}).

Table 1 summarize the ranges of variation of K, n and μ the experimental viscosity at 50 s^{-1} of mango purees at different stages of maturity. To ensure the clarity of results concerning rheological properties of purees, authors presented results according to 5 stages of maturity, *a priori* ([0-5 days], [6-10 days], [11-15 days], [16-20 days], [21-25 days]). As expected, shear-thinning behavior of all purees was confirmed by the flow behavior indexes as they presented all values below 1 ($n < 1$). It can be noticed that the flow behavior indexes (n) decreased clearly as the maturation stage of mango increased whereas the consistency indexes (K) and the dynamic viscosity (μ) noticeably decreased only when comparing purees at very early and other stages of maturation. Indeed, consistency indexes were higher when considering purees at maturity stage between 0 and 5 days and slightly decreased for the other maturation stages. All these results highlight the effect of the fresh mango maturation on its puree's viscosity. This is in line with the hydrolysis of protopectins, a binding substance between cell walls and the degradation of starch, etc. (Sánchez-gimeno, 2009) occurring during maturation and inducing a decrease of the size of suspended insoluble particles, thus, leading to a decrease of the viscosity of mango puree (Espinosa et al., 2011).

Maturity stages (Days)	Range of variation of the flow index n	Range of variation of the consistency index K (Pa.s^n)	Range of variation of the viscosity μ (Pa.s)
0 - 5	0.08 - 0.14	77 - 140	2.28 - 3.69
6 - 10	0.08 - 0.11	81 - 118	1.95 - 2.67
11 - 15	0.07 - 0.13	75 - 105	2.08 - 2.44
16 - 20	0.05 - 0.08	77 - 94	2.04 - 2.60
21 - 25	0.04 - 0.07	73 - 83	1.78 - 2.24

*For all data the given are the average of three trials and all standard deviation values are inferior to 5% of the average value.

Table 1. The ranges of variation of K, the consistency index (Pa.s^n), n, the flow behavior index and μ (Pa.s) the experimental dynamic viscosity at 50 s^{-1} of mango purees.

Fig. 7 point up a decreasing trend between the experimental dynamic viscosity at 50 s^{-1} (μ) of mango puree and the firmness of the whole fruit (D_{5N}) mainly when comparing early maturation stages [0-5 days] and [6-10 days] with the other stages. This observation emphasizes the impact of mango firmness at early stages of maturation not only on particles size of purees but also on their viscosity even if the correlation between μ and D_{5N} is not as good as for D [3;2].

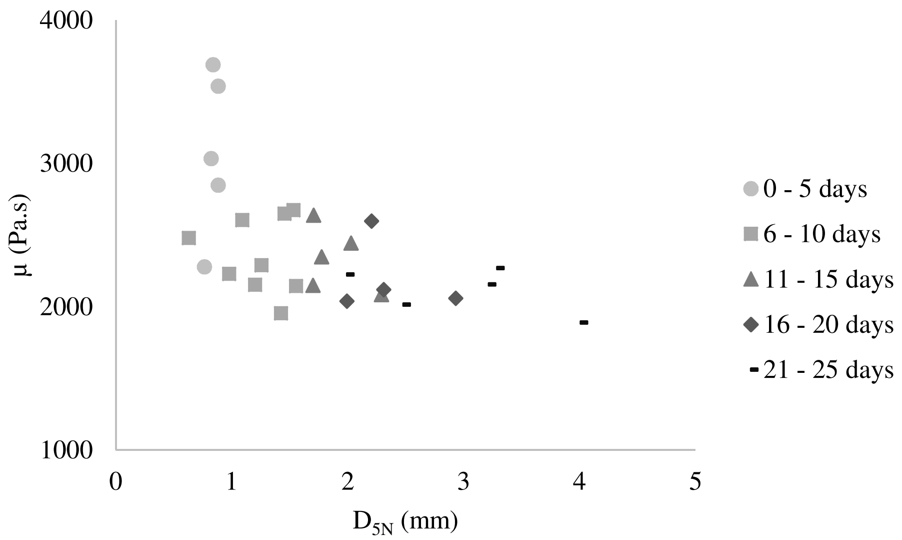

Fig. 7. Variation of the experimental dynamic viscosity μ *at 50* s^{-1} (Pa. s) as function of the D_{5N} (mm).

3.2.2.2 Oscillatory Strain Sweep

The viscoelastic behavior of different mango purees was evaluated through an oscillatory strain sweep test. For all purees the storage modulus G' and the loss modulus G" were constant in the domain of low strain amplitude (< 1%) and characterized a linear viscoelastic region (LVE-R). In this region, the storage modulus was higher than the loss modulus, showing a viscoelastic solid-like behavior. This behavior was independent of the maturity stage since all purees showed similar trends. G' and G" values declined and when a specific strain was reached, G" exceeded G' indicating a transition from a solid-like (G' > G") to a viscous-like (G" > G') behavior and a dependency of the rheological properties of purees on the strain. These results showed that, all purees can be considered as viscoelastic solids in the domain of low strain amplitude (< 1%) and viscoelastic liquids for higher strain amplitude.

Althought, all purees showed a viscoelastic solid-like behavior, a decrease in the storage modulus G' within the linear viscoelastic region (LVE-R) with maturity was observed indicating a significant decrease of the solid-like behavior of mango purees during maturation (Fig. 8 (a)). Indeed, the storage modulus of mango purees decreased significantly by 70%

before 15 days of maturation whereas beyond this maturation stage, G' was almost steady. These results show a decrease of the solid-like behavior of mango purees during maturation which is consistent with the loss of mango firmness (D_{5N}, F_{max}) and the loss of flesh solid-like behavior (G'). This observation highlights that the loss of mango firmness has an impact on the viscoelastic properties of the mango puree.

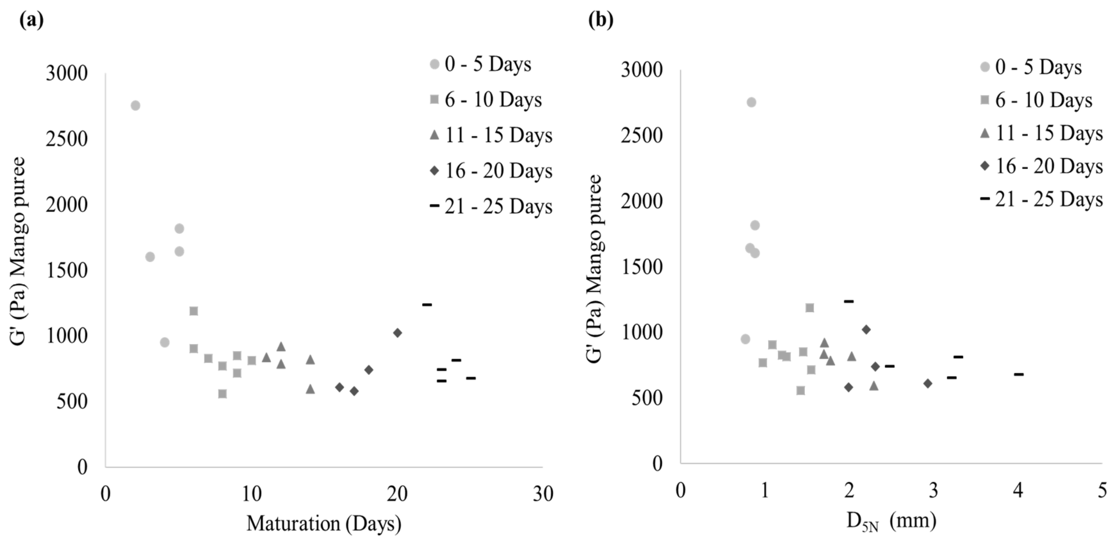

Fig. 8. Evolution of the storage modulus G' (Pa) as function of (a) the maturation (days) and (b) the D_{5N} (mm).

As for viscosity, Fig. 8 (b) shows a similar decreasing trend between for the solid-like behavior of mango puree (G') and the firmness of the whole fruit (D_{5N}), mainly when comparing early maturation stages [0-5 days] and [6-10 days] with the other stages. This observation confirmed the impact of mango firmness at early stages of maturation on the rheological properties of mango puree.

3.2.3 Physico-chemical analyses

Several physico-chemical characteristics of mango purees were assessed during maturation. In this study, the titratable acidity (TA, g citric acid/100g of puree) of mango purees decreased overall during maturation. Indeed, TA values were significantly higher for mangos in stages [0-5 days] and [6-10 days] than for the other stages as presented in Fig. 9. This decrease is in accordance with literature and could be explained by metabolic reactions including respiration in which organic acids are used as substrates (Gill et al., 2017; Lawson et al., 2019). After 15 days of maturation, no significant decrease of titratable acidity was observed showing that no more significant degradation of organic acids occurred after this maturation stage. Concerning TSS and DM of purees, no significant changes regarding these parameters were noticed before 20 days of maturation as presented in Fig. 9 (b). This observation is not in accordance with literature since several studies showed an increase in sugar content (hydrolysis of starch) and dry matter (loss in water) during maturation (Dea et al., 2013; Elbandy et al., 2014; Maldonado-Celis et al., 2019; Palafox-Carlos et al., 2012). This result could be explained by the fact that, in this study, TSS and DM of mango purees reached their highest values even at green stages [0-5 days], showing that these two parameters have evolved during storage of mango before purchasing (mango have been stored at 10°C before purchasing). Indeed, for this mango variety (*Mangifera indica* cv. Kent), several works reported that the highest values of TSS are around 20° Bx (Jha et al., 2007). After 20 days of maturation, DM and TSS decreased significantly, highlighting the degradation of sugars. These observations could be explained by the fermentation phenomenon occurring at very late stages of maturation (after 20 days) during which the sugars are consumed and volatile compounds are generated. Moreover, the evaporation of volatile compounds (ethanol) during fermentation could explain the DM decrease.

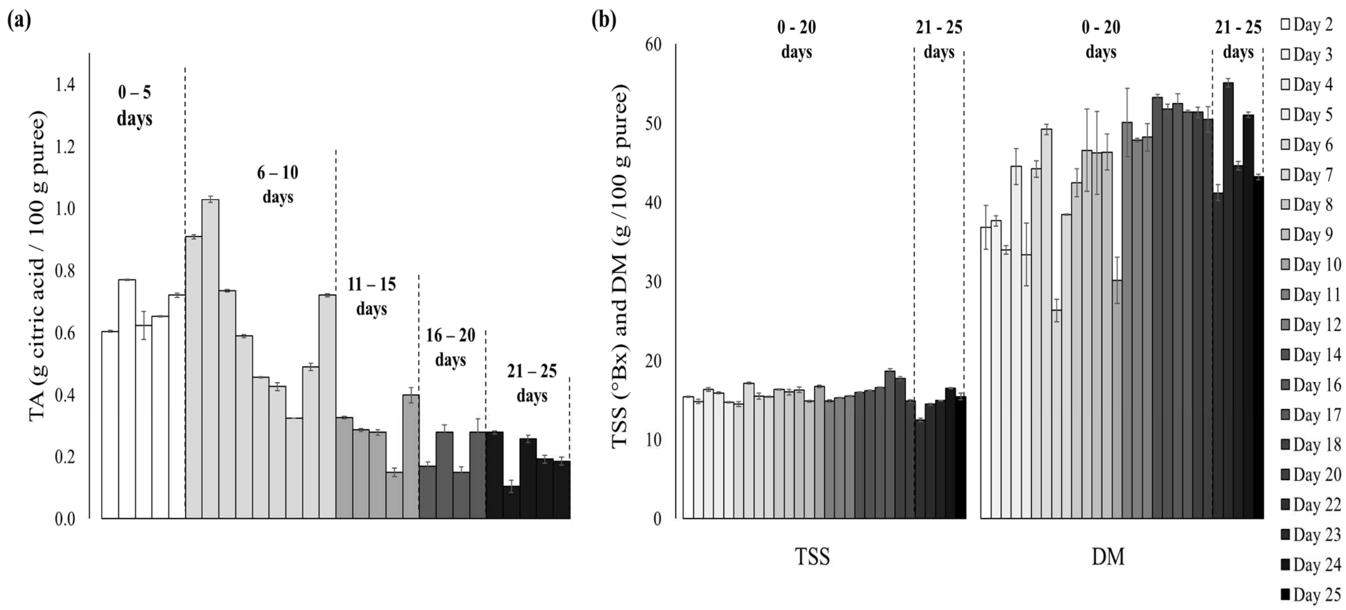

Fig. 9. Variation of (a) the titratable acidity, TA (g citric acid / 100g puree) and (b) the total soluble solids, TSS (°Bx) and dry matter, DM (g / 100g puree) during maturation.

3.2.4 Fresh mango heterogeneity and purees characteristics

Principal Component Analysis (PCA) was performed in order to visualize the total variability of characteristics of fresh mangos and mango purees.

As presented in Fig. 10 (a), about 80% of the variation in the data related to fresh mango was explained by the first two components PC 1 (64.43%) and PC 2 (15%). PC 1 is positively correlated with L*, F_{max} and G' of mango flesh and negatively correlated with D_{5N} of mango.

The second component (PC 2) is negatively correlated with the weight, density and b* and positively correlated with the G' of the mango flesh.

The projection of the 28 mangos on component PC 1 of the PCA confirmed that mangos at maturation stages below 10 days (right side of the PC 1) were mainly characterized by higher values of G', F_{max} and L* and lower values of D_{5N} and a* which is in accordance with the previous results where green mangos presented high firmness and solid-like behavior as well as lighten flesh color (Fig 10 (a)). Contrariwise, the PCA highlighted that mangos at very late maturation stage (above 20 days) were mainly characterized by the highest D_{5N} and a* values and low F_{max}, G' and L* values confirming their loss of firmness and solid-like behavior and their darker color. Concerning intermediate stages of maturation (between 10 and 20 days), they were concentrated on the center of the biplot. No further trends are noticeable when considering PC 2 information.

As shown in Fig. 10 (b), about 79% of the variation in the data related to mango purees was explained by the first two components PC 1 (59.31%) and PC 2 (19.59%). PC 1 is positively correlated with the particles size distribution, titratable acidity (TA) and rheological behavior of mango purees. Indeed, statistical diameters provided 54% whereas TA, G' and K contributed only to 9% each of the PC 1 information. The second component (PC 2) is positively correlated with the TSS and DM (65% of PC 2 information) and negatively with the G" (12.6% information of PC 2).

The projection of the 28 purees onto component PC 1 of the PCA allowed to distinguish purees from mangos at very early maturation stage (below 5 days) due to their highest values of D [3;2], D [4;3], D_{10}, D_{50}, D_{90}, TA and G'. These observations are in line with the previous results showing that green stages mango purees were characterized by the highest particles size, titratable acidity and solid-like behavior of purees Fig. 10(b). As for PC 2 component, the projection of the 28 purees enabled to discriminate purees from mango at very late maturation stage (above 20 days) mainly characterized by the lowest TSS and DM. It should be noticed that neither the projection on PC 1 nor on PC 2 allowed discriminating clearly the other stages of maturation (between 5 and 20 days).

To sum up, the studied variables for fresh mangos and mango purees allowed discriminating in both cases fresh mangos and mango purees into 3 main groups according to their maturation stages: early, intermediate and late maturation stage. In this study, mangos at early stages of maturation could be distinguished by their high firmness, solid-like behavior, viscosity and particles size whereas mangos at very late maturation stage are mainly characterized by low values of total soluble solids and dry matter. Furthermore, PCA results allowed identifying relevant indicators to (i) characterize the heterogeneity of fresh mangos and mango purees and (ii) discriminate these products according to their stage of maturation. Finally, results of PCA confirmed the main trends obtained previously when considering the evolution of each variable separately as function of maturation.

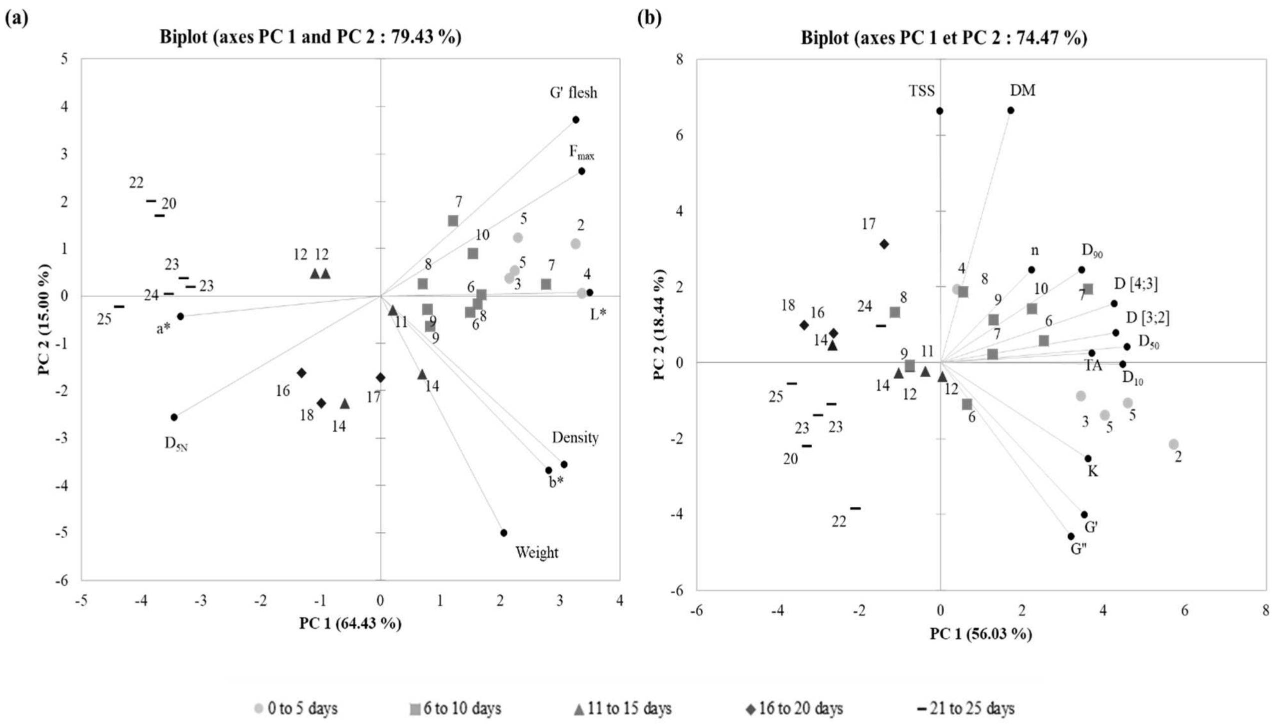

Fig. 10. **Principal component analysis (PCA)** on instrumental indicators of (a) mangos and (b) purees at different maturity stages. **a*:** red to green transition , **b*:** blue to yellow transition, **DM:** dry matter (g / 100 g puree), **D_{5N}:** distance of compression at 5N (mm), **D [3;2]:** Sauter mean diameter (µm), **D [4,3]:** Brouckere mean diameter (µm), **D_{10}, D_{50} and D_{90}:** particle size statistical diameters (µm), **F_{max}:** maximum value of the peak force (N) , **G':** storage modulus (Pa), **G":** loss modulus (Pa), **K:** consistency index (Pa.s^n), **L***: lightness (black to white transition), **n**: flow behavior index, **TA:** titratable acidity (g citric acid/ 100 g puree), **TSS:** total soluble solids (°Bx).

4. Conclusion

The aim of this study consisted in developing innovative tools for sorting mangos according to their maturity stages and to the specific properties of their purees. Instrumental characterization of fresh mangos and mango purees were carried out to identify relevant indicators of mangos heterogeneity and purees variability. Results showed that mango firmness is a great indicator of mango maturity and has an important impact on the properties of mango purees. In this work, a non-destructive compression test was proposed to measure accurately the loss of mango firmness during maturation without damaging the fruits. This fast and easy measurement allowed also to trace-back the solid-like behavior of mango measured by destructive rheological analysis. In addition, results indicated that the firmness of fresh mangos governed the particles size distributions and the rheological properties of mango purees. According to these observations, it was possible to predict the particles size of the mango purees based on the firmness of the fresh mangos. Concerning, purees rheological properties (viscosity and solid- like behavior), compression test enabled discriminating mainly mango purees at early stages of maturation [0-10 days] from the other stages [10-25 days].

PCA results confirmed that the investigated variables in this work (textural, rheological, physical and physico-chemical) seem to be good indicators to characterize the heterogeneity of fresh mangos and mango purees. It was possible to discriminate mango and puree into 3 main groups (early maturation stages, intermediate stages and a late maturation stage) based mainly on total soluble solids, dry matter, firmness, particles size and rheological properties.

This work provided new knowledge in mango field and an innovative and simple tool to sort mango according to firmness in relation with their maturity stage. This tool could be also of great interest to anticipate the characteristics of mango puree according to mango firmness. As the proposed compression test is fast and easy to perform, this sorting strategy could be easily applied not only for mango fruits but also for many other juicy stone fruits in transformation units to reduce post-harvest losses.

Formatting of funding sources

Funding: this work was carried out as part of “Interfaces” flagship project, publicly funded throught ANR (the French National Research Agency) under the “Investissements d’avenir” program with the reference ANR-10-LABX-001-01 Labex Agro and coordinated by Agropolis Fondation under the reference ID 1603-001.

References

Azira, T.N., Man, Y.B.C., Mohd, R.N.R., Aina, M.A., Amin, I., 2014. Use of principal component analysis for differentiation of gelatine sources based on polypeptide molecular weights. Food Chem. 151, 286–292. https://doi.org/10.1016/j.foodchem.2013.11.066

Boateng, C.N., 2016. Analysis of Post Harvest Losses in the Mango Marketing Channel in Southern Ghana 99.

Chantalak, T., Robert E, P., 2017. Handbook of Mango Fruit. Handb. Mango Fruit 17–35. https://doi.org/10.1002/9781119014362

Dahdouh, L., Wisniewski, C., Kapitan-Gnimdu, A., Servent, A., Dornier, M., Delalonde, M., 2015. Identification of relevant physicochemical characteristics for predicting fruit juices filterability. Sep. Purif. Technol. 141, 59–67. https://doi.org/10.1016/j.seppur.2014.11.030

Dahdouh, L., Wisniewski, C., Ricci, J., Vachoud, L., Dornier, M., Delalonde, M., 2016. Rheological study of orange juices for a better knowledge of their suspended solids interactions at low and high concentration. J. Food Eng. 174, 15–20. https://doi.org/10.1016/j.jfoodeng.2015.11.008

Dea, S., Brecht, J.K., do Nascimento Nunes, M.C., Baldwin, E.A., 2013. Optimal ripeness stage for processing “Kent” mangoes into fresh-cut slices. Horttechnology 23, 12–23. https://doi.org/10.21273/horttech.23.1.12

Djioua, T., Avignon, U.D., Des, E.T., Vaucluse, P.D.E., Coudret, M.A., Ducamp-collin, M.M.N., Reynes, M.M., Charles, M.F., 2010. Amélioration de la conservation des mangues 4 ème gamme par application de traitements thermiques et utilisation d ’ une co.

Elbandy, Mohamed A, Elbandy, M A, Abed, S.M., Gad, S.S.A., Abdel-Fadeel, M.G., 2014. Aloe vera Gel as a Functional Ingredient and Natural Preservative in Mango Nectar. World J. Dairy Food Sci. 9, 191–203. https://doi.org/10.5829/idosi.wjdfs.2014.9.2.1139

Ellong, E.N., Adenet, S., Rochefort, K., 2015. Physicochemical, Nutritional, Organoleptic Characteristics and Food Applications of Four Mango (<i>Mangifera indica</i>) Varieties. Food Nutr. Sci. 06, 242–253.

https://doi.org/10.4236/fns.2015.62025

Espinosa-muñoz, L., Renard, C.M.G.C., Symoneaux, R., Biau, N., Cuvelier, G., 2013. Structural parameters that determine the rheological properties of apple puree 119, 619–626. https://doi.org/10.1016/j.jfoodeng.2013.06.014

Espinosa, L., To, N., Symoneaux, R., Renard, C.M.G.C., Biau, N., Cuvelier, G., 2011. Effect of processing on rheological, structural and sensory properties of apple puree. Procedia Food Sci. 1, 513–520. https://doi.org/10.1016/j.profoo.2011.09.078

Evans, E.A., Ballen, F.H., Siddiq, M., 2017. Mango Production, Global Trade, Consumption Trends, and Postharvest Processing and Nutrition. Handb. Mango Fruit Prod. Postharvest Sci. Process. Technol. Nutr. 1–16. https://doi.org/10.1002/9781119014362.ch1

FAO, 2019, 2019. Mango* production worldwide from 2000 to 2017 (in million metric tons) [WWW Document]. Stat. Portal Stat. Stud. from more than 22,500 Sources. URL https://www.statista.com/statistics/577951/world-mango-production/

Gentile, Carla, Gregorio, E. Di, Stefano, V. Di, Mannino, G., Perrone, A., Avellone, G., Sortino, Giuseppe, Inglese, P., Farina, V., Gentile, C, Gregorio, D., Stefano, D., Mannino, V., Sortino, G, 2018. Food quality and nutraceutical value of nine cultivars of mango (Mangifera indica L.) fruits grown in Mediterranean subtropical environment. Food Chem. 277, 471–479. https://doi.org/10.1016/j.foodchem.2018.10.109

Gill, P.P.S., Jawandha, S.K., Kaur, N., Singh, N., 2017. Physico-chemical changes during progressive ripening of mango (Mangifera indica L.) cv. Dashehari under different temperature regimes. J. Food Sci. Technol. 54, 1964–1970. https://doi.org/10.1007/s13197-017-2632-6

Gundurao, A., Ramaswamy, H.S., Ahmed, J., 2011. Effect of soluble solids concentration and temperature on thermo-physical and rheological properties of mango puree. Int. J. Food Prop. 14, 1018–1036. https://doi.org/10.1080/10942910903580876

Jha, S.N., Chopra, S., Kingsly, A.R.P., 2007. Modeling of color values for nondestructive evaluation of maturity of mango. J. Food Eng. 78, 22–26. https://doi.org/10.1016/j.jfoodeng.2005.08.048

Joas, J., Caro, Y., Lechaudel, M., 2009. Postharvest Biology and Technology Comparison of postharvest changes in mango (cv Cogshall) using a Ripening class index (Rci) for different carbon supplies and harvest dates 54, 25–31. https://doi.org/10.1016/j.postharvbio.2009.04.008

Lawson, T., Lycett, G.W., Ali, A., Chin, C.F., 2019. Characterization of Southeast Asia mangoes (Mangifera indica L) according to their physicochemical attributes. Sci. Hortic. (Amsterdam). 243, 189–196. https://doi.org/10.1016/j.scienta.2018.08.014

Lee, M.-R., 2018. Erratum to: Objective Measurements of Textural and Rheological Properties of Cheese. J. Milk Sci. Biotechnol. 36, 186–186. https://doi.org/10.22424/jmsb.2018.36.3.186

Leverrier, C., Almeida, G., Espinosa-Mu noz, L., Cuvelier, G., 2016. Influence of Particle Size and Concentration on Rheological Behaviour of Reconstituted Apple Purees. Food Biophys. 11, 235–247. https://doi.org/10.1007/s11483-016-9434-7

Liu, F.X., Fu, S.F., Bi, X.F., Chen, F., Liao, X.J., Hu, X.S., Wu, J.H., 2013. Physico-chemical and antioxidant properties of four mango (Mangifera indica L.) cultivars in China. Food Chem. 138, 396–405. https://doi.org/10.1016/j.foodchem.2012.09.111

Lopez-Sanchez, P., Chapara, V., Schumm, S., Farr, R., 2012. Shear Elastic Deformation and Particle Packing in Plant Cell Dispersions. Food Biophys. 7, 1–14. https://doi.org/10.1007/s11483-011-9237-9

Maldonado-Celis, M.E., Yahia, E.M., Bedoya, R., Landázuri, P., Loango, N., Aguillón, J., Restrepo, B., Guerrero Ospina, J.C., 2019. Chemical Composition of Mango (Mangifera indica L.) Fruit: Nutritional and Phytochemical Compounds. Front. Plant Sci. 10, 1–21. https://doi.org/10.3389/fpls.2019.01073

Masud Parvez, G., 2016. Pharmacological Activities of Mango (Mangifera Indica): A Review. J. Pharmacogn. Phytochem. JPP 1, 1–7.

Memon, A., Marri, M.Y.K., Khushk, A.M., 2013. Estimation of mango post harvest losses in sindh 2827–2832.

Nambi, V.E., Thangavel, K., Rajeswari, K.A., Manickavasagan, A., Geetha, V., 2016. Texture and rheological changes of Indian mango cultivars during ripening. Postharvest Biol. Technol. 117, 152–160. https://doi.org/10.1016/j.postharvbio.2016.02.009

Padda, M.S., do Amarante, C.V.T., Garcia, R.M., Slaughter, D.C., Mitcham, E.J., 2011. Methods to analyze physico-chemical changes during mango ripening: A multivariate approach. Postharvest Biol. Technol. 62, 267–274. https://doi.org/10.1016/j.postharvbio.2011.06.002

Palafox-Carlos, H., Yahia, E., Islas-Osuna, M.A., Gutierrez-Martinez, P., Robles-Sánchez, M., González-Aguilar, G.A., 2012. Effect of ripeness stage of mango fruit (Mangifera indica L., cv. Ataulfo) on physiological parameters and antioxidant activity. Sci. Hortic. (Amsterdam). 135, 7–13. https://doi.org/10.1016/j.scienta.2011.11.027

Penchaiya, P., Uthairatanakij, A., Srilaong, V., Kanlayanarat, S., Tijskens, L.M.M., Tansakul, A., 2015. Measurement of mango firmness by non-destructive limited compression technique. Acta Hortic. 1088, 73–78. https://doi.org/10.17660/ActaHortic.2015.1088.7

Phaokuntha, S., Poonlarp, P.B., Pongsirikul, I., 2014. Rheological properties of mango puree and process development of mango sheet. Acta Hortic. 1024, 373–380.

Pronprasit, R., Natwichai, J., 2013. Prediction of Mango Fruit Quality from NIR Spectroscopy using an Ensemble Classification. Int. J. Comput. Appl. 83, 25–30. https://doi.org/10.5120/14517-2903

Rivier, M., Méot, J.-M., Ferré, T., Briard, M., 2009. Le séchage des mangues. Le séchage des mangues. https://doi.org/10.35690/978-2-7592-0342-0

Rumainum, I.M., Worarad, K., Srilaong, V., Yamane, K., 2018. Fruit quality and antioxidant capacity of six Thai mango cultivars. Agric. Nat. Resour. 52, 208–214. https://doi.org/10.1016/j.anres.2018.06.007

Sánchez-gimeno, A.N.A.C., 2009. White guava fruit and purees : textural and rheological properties and effect on the temperature 40, 334–345.

Valente, M., Ribeyre, F., Self, G., Berthiot, L., Assemat, S., 2011. Instrumental and sensory characterization of mango fruit texture. J. Food Qual. 34, 413–424. https://doi.org/10.1111/j.1745-4557.2011.00412.x

Venkatesan, T., Tamilmani, C., 2013. Effect of Ethrel on the Starch Sugar Changes of Off-Season Fruits of Mango (M*angifera indica* l. Var. Neelum) during Ripening. Int. Lett. Nat. Sci. 7, 1–12. https://doi.org/10.18052/www.scipress.com/ilns.7.1

Yashoda, H.M., Prabha, T.N., Tharanathan, R.N., 2006. Mango ripening: Changes in cell wall constituents in relation to textural softening. J. Sci. Food Agric. 86, 713–721. https://doi.org/10.1002/jsfa.2404

Zakaria, A., Md Shakaff, A.Y., Masnan, M.J., Saad, F.S.A., Adom, A.H., Ahmad, M.N., Jaafar, M.N., Abdullah, A.H., Kamarudin, L.M., 2012. Improved maturity and ripeness classifications of Magnifera Indica cv. harumanis mangoes through sensor fusion of an electronic nose and acoustic sensor. Sensors (Switzerland) 12, 6023–6048. https://doi.org/10.3390/s120506023

Graphical abstract